


# Simulation of space heavy-ion induced primary knock-on atoms in bipolar devices

Bin Zhang(张彬), Hao Jiang(姜昊), Xiao-Dong Xu(徐晓东), Tao Ying(应涛), Zhong-Li Liu(刘中利), Wei-Qi Li(李伟奇), Jian-Qun Yang(杨剑群), and Xing-Ji Li(李兴冀)

**Citation:**Chin. Phys. B, 2024, 33 (**1**): 016106. DOI: 10.1088/1674-1056/acd3e1

Journal homepage: http://cpb.iphy.ac.cn; http://iopscience.iop.org/cpb

**What follows is a list of articles you may be interested in**

---

## Angular dependence of proton-induced single event transient in silicon-germanium heterojunction bipolar transistors

Jianan Wei(魏佳男), Yang Li(李洋), Wenlong Liao(廖文龙), Fang Liu(刘方), Yonghong Li(李永宏), Jiancheng Liu(刘建成), Chaohui He(贺朝会), and Gang Guo(郭刚)

Chin. Phys. B, 2022, 31 (**8**): 086106. DOI: 10.1088/1674-1056/ac5d32

## Influence of helium on the evolution of irradiation-induced defects in tungsten: An object kinetic Monte Carlo simulation

Peng-Wei Hou(侯鹏伟), Yu-Hao Li(李宇浩), Zhong-Zhu Li(李中柱), Li-Fang Wang(王丽芳), Xingyu Gao(高兴誉), Hong-Bo Zhou(周洪波), Haifeng Song(宋海峰), and Guang-Hong Lu(吕广宏)

Chin. Phys. B, 2021, 30 (**8**): 086108. DOI: 10.1088/1674-1056/abf7ac

## Magnetic properties of $La_2CuMnO_6$ double perovskite ceramic investigated by Monte Carlo simulations

S Mtougui, I EL Housni, N EL Mekkaoui, S Ziti, S Idrissi, H Labrim, R Khalladi, L Bahmad

Chin. Phys. B, 2020, 29 (**5**): 056101. DOI: 10.1088/1674-1056/ab7d95

## Geant4 simulation of proton-induced single event upset in three-dimensional die-stacked SRAM device

Bing Ye(叶兵), Li-Hua Mo(莫莉华), Tao Liu(刘涛), Jie Luo(罗捷), Dong-Qing Li(李东青), Pei-Xiong Zhao(赵培雄), Chang Cai(蔡畅), Ze He(贺泽), You-Mei Sun(孙友梅), Ming-Dong Hou(侯明东), Jie Liu(刘杰)

Chin. Phys. B, 2020, 29 (**2**): 026101. DOI: 10.1088/1674-1056/ab5fc4

## Monte Carlo simulation of asymmetrical growth of cube-shaped nanoparticles

Yuanyuan Wang(王元元), Huaqing Xie(谢华清), Zihua Wu(吴子华), Jiaojiao Xing(邢姣娇)

Chin. Phys. B, 2016, 25 (**9**): 096104. DOI: 10.1088/1674-1056/25/9/096104

---

# Simulation of space heavy-ion induced primary knock-on atoms in bipolar devices

Bin Zhang(张彬)[1], Hao Jiang(姜昊)[2], Xiao-Dong Xu(徐晓东)[2], Tao Ying(应涛)[1], Zhong-Li Liu(刘中利)[2], Wei-Qi Li(李伟奇)[1,3], Jian-Qun Yang(杨剑群)[2], and Xing-Ji Li(李兴冀)[2,†]

[1] *School of Physics, Harbin Institute of Technology, Harbin* 150001, *China*
[2] *School of Material Science and Engineering, Harbin Institute of Technology, Harbin* 150001, *China*
[3] *State Key Laboratory of Intense Pulsed Radiation Simulation and Effect, Xi'an* 710024, *China*

(Received 23 February 2023; revised manuscript received 10 May 2023; accepted manuscript online 10 May 2023)

Bipolar junction transistors (BJTs) are often used in spacecraft due to their excellent working characteristics. However, the complex space radiation environment induces primary knock-on atoms (PKAs) in BJTs through collisions, resulting in hard-to-recover displacement damage and affecting the performance of electronic components. In this paper, the properties of PKAs induced by typical space heavy ions (C, N, O, Fe) in BJTs are investigated using Monte Carlo simulations. The simulated results show that the energy spectrum of ion-induced PKAs is primarily concentrated in the low-energy range (17 eV–100 eV) and displays similar features across all tested ions. The PKAs induced by the collision of energetic ions have large forward scattering angles, mainly around 88°. Moreover, the distribution of PKAs within a transistor as a function of depth displays a peak characteristic, and the peak position is linearly proportional to the incident energy at a certain energy range. These simulation outcomes serve as crucial theoretical support for long-term semiconductor material defect evolution and ground testing of semiconductor devices.

**Keywords:** Monte Carlo simulation, primary knock-on atom (PKA), space-heavy ion, radiation damage

**PACS:** 61.82.Fk, 61.80.Jh, 42.88.+h **DOI:** 10.1088/1674-1056/acd3e1

## 1. Introduction

The influence of space radiation on electronic components is mainly due to the total ionizing dose, displacement damage and single-event effect.[1] The radiation effects of the space radiation environment on the electronic components inside a spacecraft have attracted extensive attention.[1,2] The above-mentioned radiation effects can lead to abnormality or failure of electronic devices and eventually the failure of the mission of the orbiting spacecraft. As silicon-based devices with good current drive capability, linearity, and other operating characteristics, bipolar junction transistors (BJTs) are often used in spacecraft. However, BJTs are sensitive to cosmic rays and may suffer displacement damage during on-orbit missions.[2–4]

Displacement damage is caused by energetic particles colliding with target material atoms, resulting in the dislodging of atoms from their lattice position.[5] Displacement damage is hard to recover, which will seriously affect the electrical performance and lead to the degradation of semiconductor devices.[6,7] Primary knock-on atoms (PKAs), which are the first atoms to be displaced, usually have a higher energy level that can result in further cascade damage. Much work has been done on cascading damage in past studies, mainly on the microscopic mechanisms of displacement damage, to replace empirical methods such as non-ionizing energy loss (NIEL).[8–10] For example, using molecular dynamics (MD) simulation, He *et al.*[6] studied the relationship of temperature with primary damage and found that temperature could increase the fraction of isolated vacancies in vacancy clusters because vacancy clusters may be thermally unstable. Hamedani *et al.*[11] performed a comparative study of different materials to examine the damage production mechanisms for a relatively wide range of materials and recoil energies. The above-mentioned MD simulation works were generally to select PKA incident materials with specific energy artificially to study the damage process of semiconductors. Researchers are trying to link the macroscopic electrical effects observed in the experiments with the microscopic damage structures generated at the atomic level,[12] and are attempting to combine different simulation techniques (e.g., Monte Carlo, MD, *ab initio*). Obtaining a wealth of information on PKAs is crucial in this process. Researchers have extensively studied the PKAs generated by irradiated particles in materials. For example, Liu *et al.*[13] investigated radiation damage in a silicon drift detector (SDD) and found that the distribution of displacement damage caused by neutrons in SDDs is uniform. Shen *et al.*[14] studied the non-ionization energy loss of protons in silicon carbide and found that with an increase in incident proton energy the proportion of Si and C particles in the primary recoil atoms gradually decreased, from primary products to secondary products.

Previous studies have primarily focused on radiation damage to materials by neutrons and protons. However, there

†Corresponding author. E-mail: lxj0218@hit.edu.cn

© 2024 Chinese Physical Society and IOP Publishing Ltd 

are few reports on the PKAs induced by space heavy ions in semiconductors, despite heavy ions being common radiation particles in outer space and ground radiation sources. The simulation of PKAs induced by space heavy ions in semiconductors has important application scenarios and practical significance. In addition, the rich PKA information obtained by simulations can be used as important MD reference input parameters. Therefore, this study uses Monte Carlo simulation to study the PKAs induced by heavy ions in BJTs and qualitatively analyzes the radiation damage of typical space heavy ions in semiconductor materials. This research is of great significance as it provides a better understanding of the process of displacement damage caused by charged heavy ions in semiconductors.

## 2. Models and physical processes

### 2.1. Model setup

In our previous research,[2] we conducted an experimental study on the NPN BJT 2N2222. The thickness of the base (p+) and epitaxial layer (n−) of the 2N2222 BJT is about 1.5 μm and 10 μm, respectively. In this simulation, we reduced the 2N2222 BJT to bulk Si cubes with dimensions of 10 μm × 10 μm × 10 μm, focusing on the simulation of intrinsic Si, which is similar to a previous study.[12] In addition, to studying the distribution of PKAs in the BJT as a function of depth, the Si bulk material was divided into 100 parts vertically to count the number of PKAs in each layer. The model diagram is shown in Fig. 1.

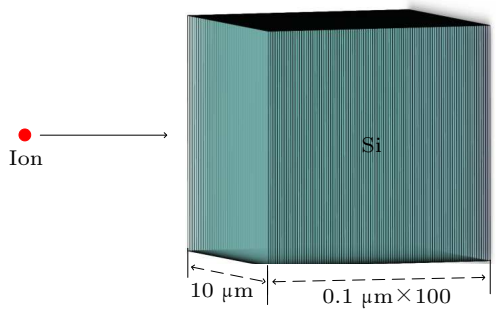



**Fig. 1.** The direction of ion incidence and the model of BJTs in this study. 2N2222 BJTs were simplified as Si bulk material with 100 layers. The length and width of each layer is 10 μm and the thickness is 0.1 μm.

### 2.2. Beam source energy setting

Galactic cosmic rays are mainly composed of light ions (protons and He) and heavy ions.[7,15] Heavy ions are found to decrease considerably in relative abundance after Fe ions in space. Hence, we conducted our simulations with ions that have an atomic number lower than Fe. The ions used in the simulation were $^{12}$C, $^{14}$N, $^{16}$O and $^{56}$Fe. Energetic ions will dissipate energy due to electronic excitation and atomic displacement in host materials. Therefore, ion energy selection in simulations is mainly based on the ion range calculated using SRIM (stopping and range of ions in matter).[16] The calculated results for the ion ranges are shown in Fig. 2. Previous studies have revealed that an increase in the energy of incident ions tends to weaken the displacement damage dose at the corresponding location within a device.[2] Therefore, in the simulation we only consider ion incidence within a certain energy range. In other words, we take the total thickness of the model BJTs (10 μm) as the maximum range of the ion and choose an appropriate energy as the ion energy used in our simulation. The selected ion kinetic energy parameters are shown in Table 1.

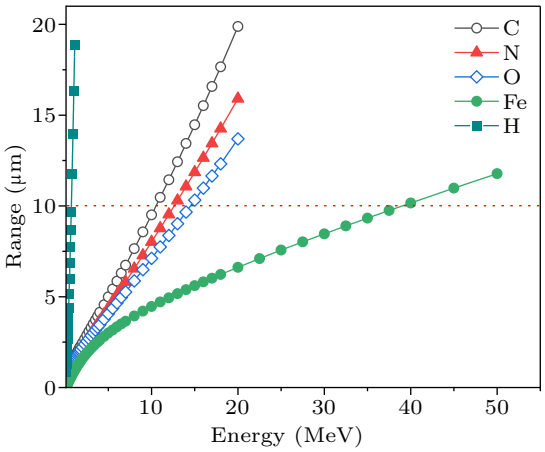



**Fig. 2.** The range of different types of ions (C, N, O and Fe) in Si bulk material. The horizontal axis represents the incident energies of ions. The red dotted line represents the total thickness of the BJTs.

**Table 1.** The types of ions used in the simulation and the ion energy chosen for this simulation

| Ion species | Energy (MeV) | | | |
|---|---|---|---|---|
| H | 0.7 | | | |
| C | 2 | 4 | 6 | 10 |
| N | 2 | 4 | 6 | 13 |
| O | 2 | 4 | 6 | 14 |
| Fe | 2 | 10 | 25 | 37 |

### 2.3. Simulation parameters

Our research work uses one module of the software Extreme-environment Radiation Effect Technology Computer Aided Design (ERETCAD) developed by the present authors, which is mainly based on GEANT4 (GEometry ANd Tracking). GEANT4[17] is an open-source simulation toolkit that offers a wide set of physics models; it has a good performance in particle transport and is also used in the field of semiconductor irradiation and medical and space applications.[18,19]

The calculation results of TRIM (transport of ions in matter) were used as the benchmark in this study.[16] TRIM is a computational subroutine of SRIM that employs Monte Carlo simulations to track the ion trajectory and determine the energy transferred to each target atom collision. In the following discussions we will refer to both SRIM and TRIM interchangeably but only use the name SRIM. After considering

the convergence of the simulations and the storage of the data, we conducted simulations up to 100000 events in our code and up to 300 events using SRIM. The number of events remained unchanged for different types of ions.

A proper physical list is crucial to obtaining accurate results of the simulation. We use a physical list called standardNR to simulate the transport of heavy ions in BJTs and the production of PKAs. A single Coulomb scattering process is included in standardNR. This physical list also explicitly integrates the classical equations of motion for scattering events, resulting in precise tracking of both the projectile and the recoil target nucleus.[20] In addition, accurate description of the transport process of heavy ions requires not only electromagnetic processes but also physical processes such as elastic and inelastic heavy ions. The physical process of the developed test application is based on the GEANT4 TestEm7 example. The NeutronHPphysics list is used to complete some neutron collision simulation studies. For the simulation of neutrons in materials, we refer to Raine *et al.*'s research work.[12] An option called 'detailed calculation with full damage cascades' was used in this simulation to achieve the accuracy of SRIM calculation results. This option follows every recoil until its energy drops below the lowest displacement energy of any target atom. Hence all collisional damage to the target is analyzed. For the extraction of PKA information in SRIM in this study we mainly refer to the research of Liu *et al.*[21]

## 3. Results and analysis

### 3.1. Energy spectrum of PKAs

The energy distribution of PKAs can provide an important parameter for semiconductor defect evolution. The first parameter extracted from simulations was the energy spectrum of the PKAs. The results of calculation from SRIM are used as a reference because of the wide acceptance of SRIM in many fields. As shown in Fig. 3, all the results are normalized to the total number of events used in this simulation.

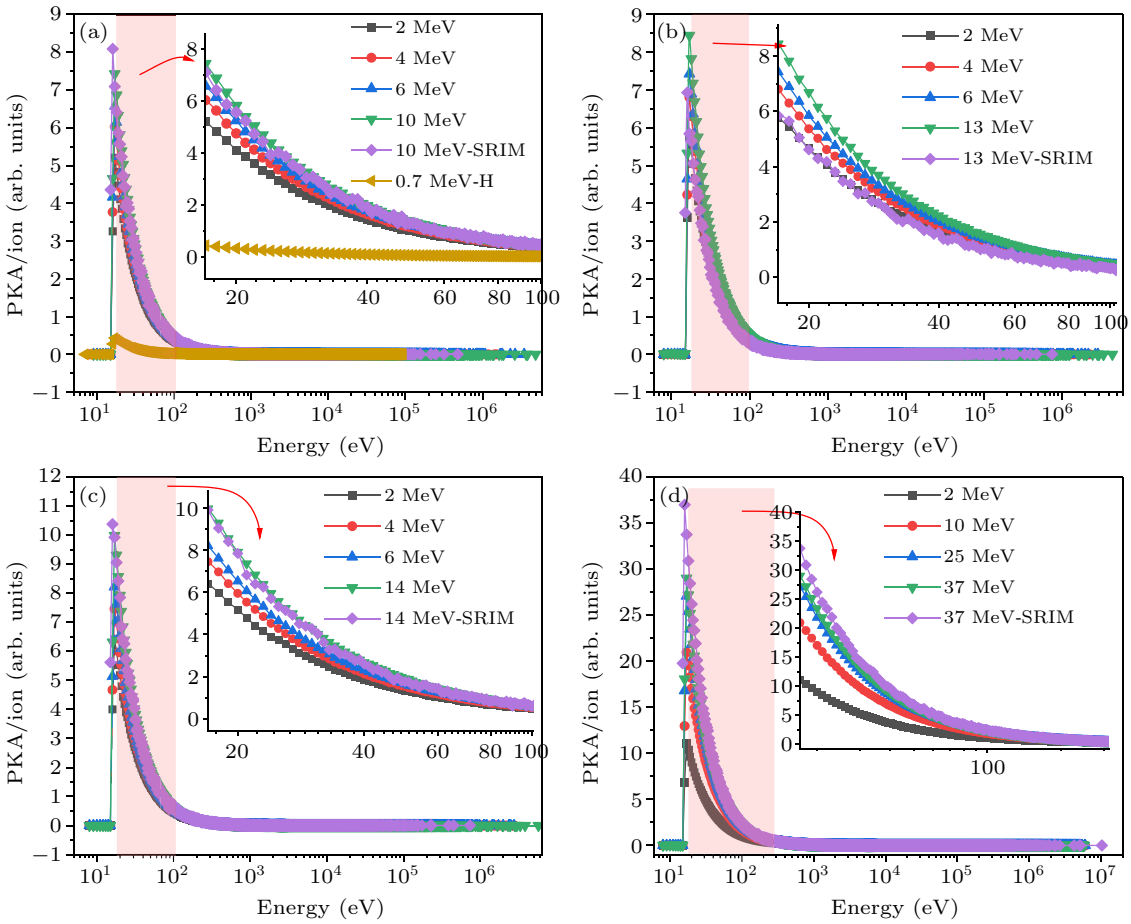



**Fig. 3.** Energy spectra of PKAs induced by different heavy ions in BJTs: (a) C, (b) N, (c) O, (d) Fe. The simulation results of SRIM are shown with purple diamonds. The results for 0.7 MeV protons are shown in panel (a). In the inset of each figure, we present the details of the PKA energy spectrum around the peak position.

As shown in Fig. 3, it is found that PKAs induced by space ions of different types and energies have a similar energy spectral distribution trend. The energy spectrum of PKAs reaches its peak at 17 eV and drops rapidly thereafter. The variation range of the energy spectrum is mainly 20 eV–100 eV and the trend of each energy spectrum is consistent after 1000 eV. PKAs have different cut-off energies according to different incident energies and types of incident ions. The

process of producing PKAs is an elastic collision process and the effects of electron excitation can be basically ignored. This process can be described by a binary collision approximation based on the conservation of momentum and energy[22]

$$E = \frac{4M_nM}{(M_n+M)^2}E_n\cos^2\theta, \tag{1}$$

where $M_n$ and $M$ are the masses of the incident ion and the target atom, $E_n$ is the energy of the incident ion and $\theta$ is the scattering angle of the recoil atom. As shown in Eq. (1), the energy attained by PKAs is affected by many factors, which is the reason why there is a maximum cut-off energy.

The amplitude of the energy spectrum is greatly affected by the incident energy and ion type. As shown in Fig. 3, we noted that the $y = ax^b$ function can better describe the change in the energy spectrum in the low-energy region (17 eV–1000 eV). In this paper, we use fitting parameters to intuitively analyze the impact of different types and energies of incident ions on the energy spectrum distribution of PKAs. To obtain a complete calculation and results analysis, ions with higher energy have also been considered in this study; the range of these ions exceeds the thickness of the BJTs (10 μm) studied in this paper. The functional relationship between fitting parameters and incident ion energy is shown in Fig. 4.

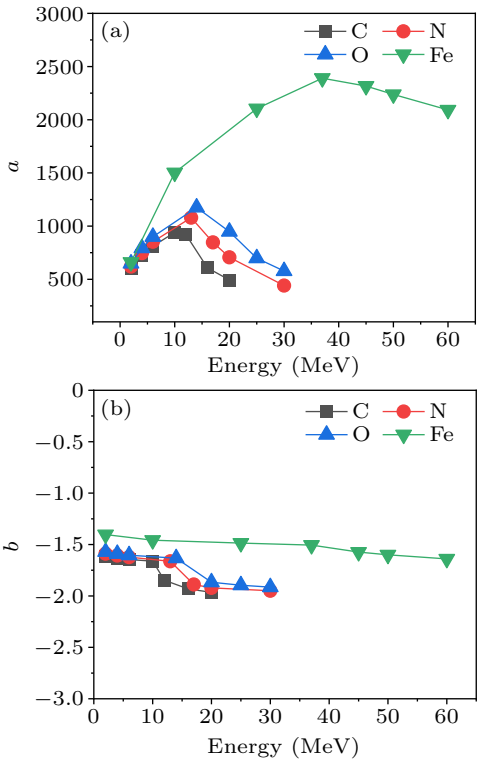



**Fig. 4.** The relationship between the fitting parameters obtained by fitting the PKA energy spectrum with functions and the incident ions energy (in the PKA energy range of 17 eV–1000 eV). (a) The fitting parameter $a$. (b) The fitting parameter $b$ as a function of the initial energy of the incident ions.

Coefficient $a$ determines the amplitude height of the function and coefficient $b$ determines the steepness of the function. As shown in Fig. 4(a), at the same incident energy coefficient $a$ is positively correlated with the atomic number (the mass of the incident ion), which means that the amplitude height of the PKA energy spectrum increases. The increase in atomic number will directly lead to an increase in the number of PKAs. This is mainly because the elastic scattering cross section of ions in a material is related to the ion mass.[7] When the range of ions is close to the size of the BJT, and reaches its maximum value, the peak height of the PKA energy spectrum reaches its maximum. However, when the ion range is larger than the size of the BJT, the number of PKAs begins to reduce. The main reason for this phenomenon is that the energy obtained by the target atom is negatively correlated with the velocity or energy of the incident ions.[23] The increase in the incident velocity of ions means that the reaction time between ions and the target decreases. Thus, the number of PKAs induced by high-energy ion incidence decreases. As shown in Fig. 4(b), the value of $b$ is less affected by the type of incident ion and its energy; the value of $b$ is maintained at a value of around −1.5. The magnitude of $b$ also determines the profile and trend of the energy spectrum, therefore the PKAs produced in BJTs by different types of ions have a similar energy spectrum distribution.

The energy spectrum of space ion-induced PKAs is mainly in the low-energy region, and PKAs with low energy will not produce cascading damage. Therefore, we believe that the characteristics of PKAs can be used to quickly and qualitatively analyze the displacement damage of space ions in BJTs. Previous MD studies have shown that larger atomic-scale structural damage is often caused by PKAs with greater energy.[6,24] In our simulation, information about high-energy PKAs was also recorded, but the probability of their generation is relatively small. Therefore, we believe that through the local simulation of these PKAs with fewer occurrences but higher energy we can complete a more complete theoretical analysis of displacement damage to semiconductor materials or devices. Finally, as shown in Fig. 3, the result of the simulation is close to those of SRIM, so we believe that the code of the simulation in this study is effective; this allows us to further investigate the nature of PKAs induced by space ions in BJTs. We attribute the variation seen between our code and SRIM in the incident scenarios of 13 MeV N ions in Fig. 3(b) and 37 MeV Fe ions in Fig. 3(c) to the distinct principles of the two calculation methods: SRIM employs the binary collision approximation method while GEANT4 is more reliant on the collision cross section.

### 3.2. PKA angle distribution

Another important characteristic of PKAs, the angle distribution, is also worthy of attention. In previous MD studies[6,11] the PKAs were mostly chosen to fall vertically. However, previous reported studies have also shown that the

incidence direction and distance of PKA may have a certain impact on the damage yield.[22,25] Therefore, the angle distribution of PKAs induced by heavy ions in BJTs was also studied in this paper. The scattering angle of PKAs was defined to be the angle between the velocity direction of the PKA and the initial direction of the incident ion. The results of the simulation are shown in Fig. 5.

The results of the simulation demonstrated that the velocity distribution of PKAs is from 0° to 180°. This is mainly because incident ions are kinds of charged particles that will be deflected by the Coulomb interaction of the target atoms during the ion transport process. Therefore, the PKAs induced by ions have the entire spatial distribution. The PKAs induced by typical heavy ions and protons in BJTs (Fig. 5(a)) had a distinct single-peak feature with a peak position around 88° and were not affected by ion type and energy. This also means that within a certain range of incident energies, the PKAs generated by the collision of heavy ions have a larger forward scattering angle. In addition, our proton irradiation results are very close to previous research conclusions. Whitlow and Nakagawa[26] calculated the angle distribution of PKAs produced by 1 MeV protons incident in Si, and their results showed that the peak position of the PKAs was around 89°. According to the binary collision theory (Eq. (1)), in the case of a larger scattering angle the energy obtained by PKAs is smaller, which is consistent with the energy spectrum distribution of PKAs obtained in our simulation. In addition, for this single-peak feature of PKA angle distribution, we have also done further research to explore whether other particle types can produce similar phenomena in BJTs. Previous studies[22] have shown that neutrons, as a typical neutral particle, can produce large displacement damage. Therefore, we investigated the neutron-induced angular distribution of PKAs in BJT. In our neutron simulation, the energy of incident neutrons can cover all physical reactions between neutrons and matter, and the simulation results are shown in Fig. 6.

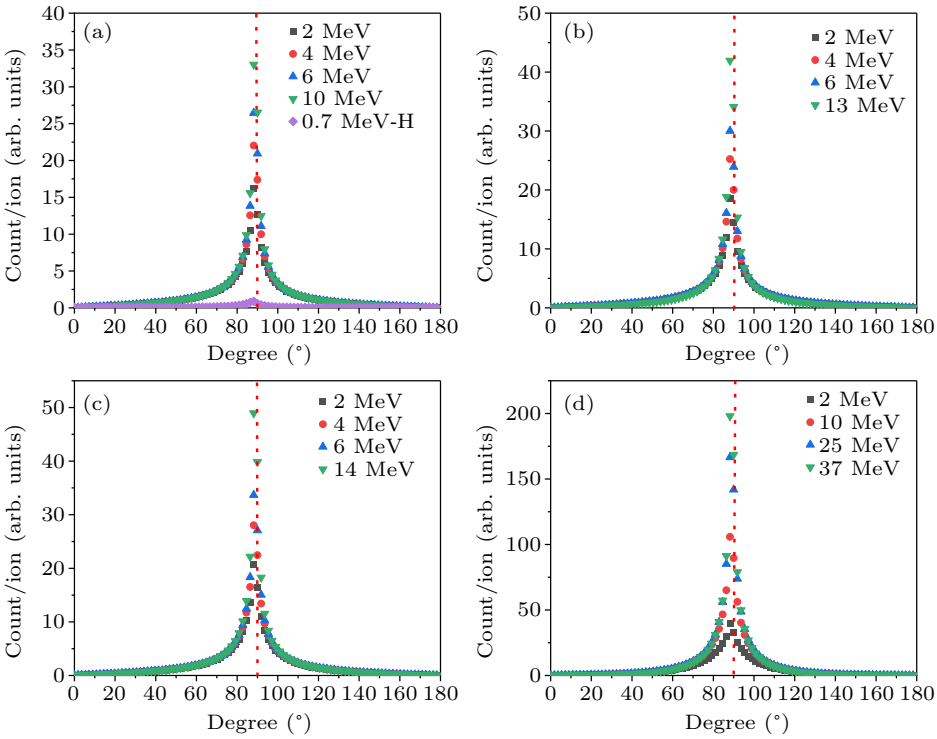



**Fig. 5.** Scattering angle distribution of PKAs induced by different heavy ions in BJTs: (a) C, (b) N, (c) O, (d) Fe. In (a) the purple symbols represent the PKA angle distribution induced by proton incidence. The red dotted line indicates that the scattering angle is 90°.

It is important to note that we did not apply the same normalization to the neutron calculations when comparing the properties of neutron and space ion-induced PKAs. This is mainly because the charged particles and neutrons use different physical models in the simulation so they can only be qualitatively compared. As shown in Fig. 6, the angular distribution of PKAs induced by neutrons can also be distributed in the entire spatial angle range. When low-energy neutrons are incident (1 MeV), the simulation results show that the angular distribution of PKAs has a wide range of peaks, and the peak position is about 64°. When neutrons with an energy of 15 MeV are incident, three angular peaks appear. The number of peaks is affected by the neutron energy. A similar phenomenon also appeared in the simulation by Cai *et al.*[22] when simulating neutron-induced PKAs in Zr-based alloys. The main reason for this phenomenon is that the interaction between neutrons and matter is accompanied by a nuclear reaction, resulting in a variety of nuclear fragments. For charged ions, the transport process of 1 MeV protons in SiC materials predicted by Shen *et al.*[14] showed that PKAs generated from nuclear re-

actions accounted for a small proportion of all PKAs. The fragmentation cross section of heavy ions is affected by the energy of the incident ions. In this study, the simulated energy of incident ions is small, and the PKAs generated come mostly from the elastic scattering process. The contribution of nuclear reactions can be ignored. Therefore, there is no multi-peak phenomenon in the angular distribution of PKAs induced by heavy ions.

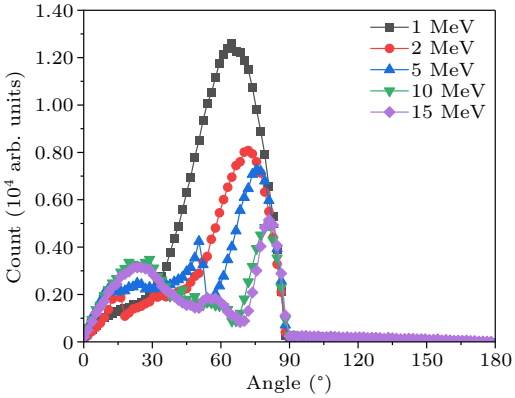



**Fig. 6.** Scattering angle distribution of PKAs induced by neutron in BJTs. A large neutron energy range is used for incidence on the BJTs, covering most of the reaction processes of neutrons and materials.

From the simulation results, it can be seen that both charged ions and neutral particles have similar scattering angle distributions in Si-based BJTs, and the PKAs have a large forward scattering angle. Therefore, we believe that when using MD to study the evolution of defects induced by heavy ions in BJTs we can choose a certain angle for the PKA incidence direction instead of just vertical incidence. In addition, it can be seen from Fig. 6 that neutron-induced PKAs in BJTs also have a large scattering angle (61°–81°). The main reason for this may be that the probability of head to head collision of particles with target atoms in the process of transmission of particles in the material is small. Charged ions are also affected by the Coulomb force, so the PKA angle induced by ions is larger. Neutral particles can produce more forward scattering.

### 3.3. The depth distribution of PKAs

The ranges of space ions with different energies vary in materials, resulting in displacement damage in varied areas of BJTs by charged ions. The localized defect evolution of BJTs can help us gain invaluable insights into the defect distribution in real irradiation environments. If the relationship between ion energy and PKA distribution in the device is established it can be used to guide ground experiments to study the effect of displacement damage in specific regions of the BJT on its electrical performance. The simulation results of PKA depth–count curves in a BJT chip are plotted in Fig. 7.

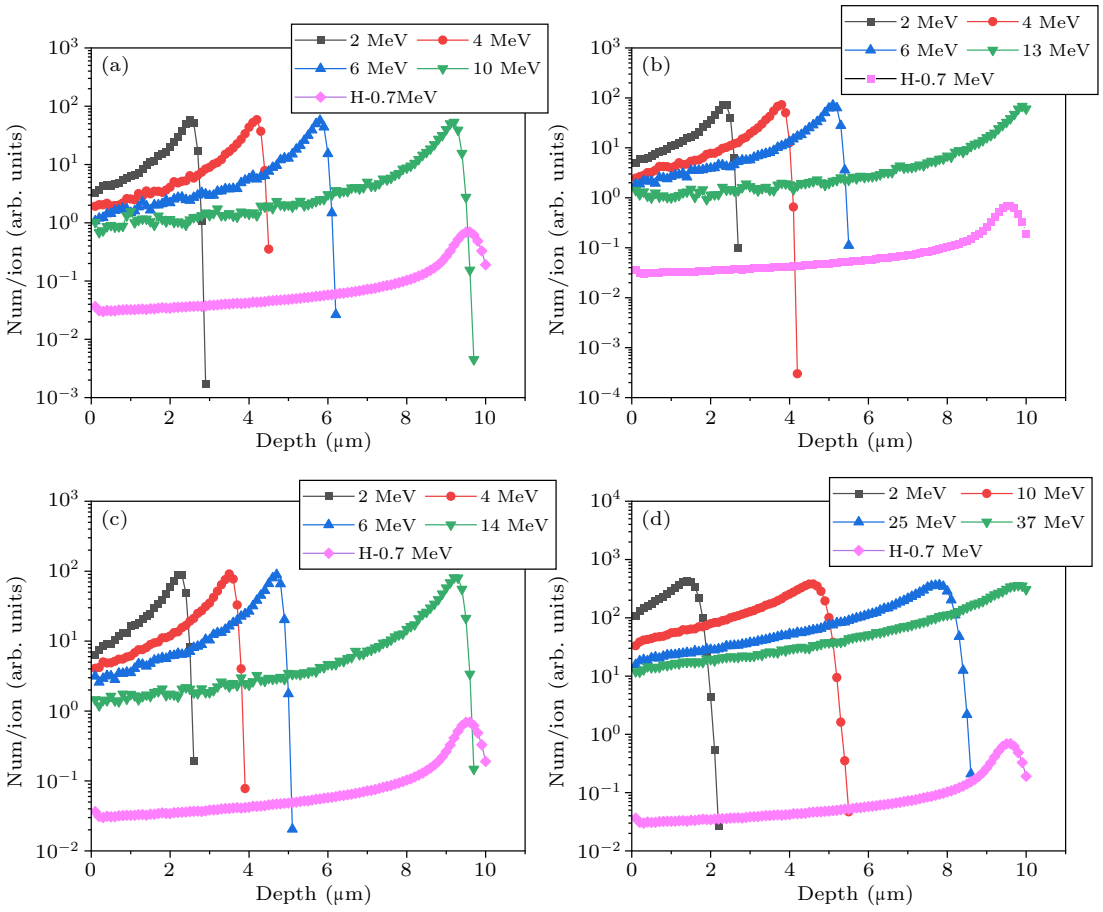



**Fig. 7.** PKA depth–count curves induced by different heavy ions in BJTs: (a) C, (b) N, (c) O, (d) Fe. The pink diamonds represent the PKAs distribution of 0.7 MeV protons in BJTs.

From the results of the simulation, it can be seen that the distribution of PKAs along the direction of the incident ions exhibits an obvious peak characteristic. The peak initially increases with increase in depth, and then decreases rapidly after reaching the peak. The displacement damage area is not evenly distributed. More displacement damage occurs near the peak position. This is because the energy loss of charged particles is characterized primarily by the square of the nuclear charge and the inverse square of the projectile velocity. Space ions are slower at the end of their range and therefore produce more PKAs. Similarly, this phenomenon also occurs at the incident position, and the number of PKAs decreases with increase in the incident particle energy. At the end of the ion range, the ion energy is not sufficient to induce PKAs, so the number of PKAs decreases rapidly.

The relationship between the peak position of PKAs and the incident ion energy is shown in Fig. 8. It can be seen from the calculation results that the depth position of the PKA peak is a linear function of the incident ion energy for the same incident ion. However, it should be noted that the peak position should occur within a certain energy range, that is, the range of ions is smaller than the thickness of the BJT. The peak position is affected by many factors, mainly the atomic number and the energy of the incident ion. At the same ion incident energy, the atomic number has a negative correlation with the peak of the incident depth.

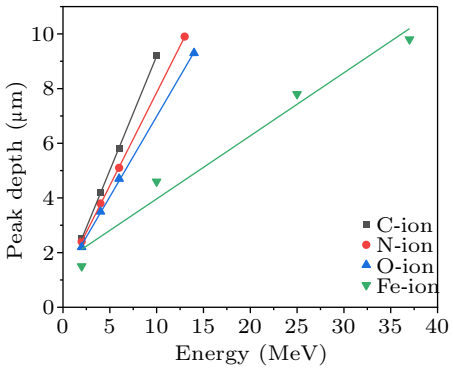



**Fig. 8.** PKA depth–count curves induced by different heavy ions in BJTs: (a) C, (b) N, (c) O, (d) Fe.

## 4. Conclusion

Monte Carlo simulation was used to compute the displacement damage induced by space ions, focusing on the properties of primary knock-on atoms (PKAs). Our results demonstrate that the properties of PKAs are mainly affected by the type and energy of incident ions. The energy spectrum of PKAs is mainly concentrated in the low-energy region, which is insufficient to cause further cascade damage. Hence the PKAs generated by ions can effectively qualitatively describe the displacement damage in a BJT. Within a certain range of ion incident energies, the distribution of ion-induced PKAs in BJT is inhomogeneous, with an objective peak distribution trend. Our calculation results show that the peak position is a function of the incident ion and energy, which allows us to study the influence of displacement damage in specific areas of BJTs on their electrical performance by adjusting the type of incident ion and incident energy. Additionally, the research results reveal that PKA chooses a certain angle of incidence and localized defect evolution to confirm the displacement damage in each area of BJT can be more consistent with the real radiation damage scenario. In summary, our work supports the investigation of displacement damage induced by space ions in BJTs and the simulation of defect evolution in semiconductor materials.

## Acknowledgments

Project supported by the National Natural Science Foundation of China (Grant Nos. 11974091, 51973046, U22B2044, and 21673025) and the Open Projects of State Key Laboratory of Intense Pulsed Radiation Simulation and Effect (Grant No. SKLIPR2020).

## References

[1] Ye B, Mo L H, Liu T, Luo J, Li D Q, Zhao P X, Cai C, He Z, Sun Y M, Hou M D and Liu J 2020 *Chin. Phys. B* **29** 26101
[2] Li X J, Yang J Q, Liu C M, Li P W, Zhao Y L and Liu G Q 2017 *IEEE Transactions on Nuclear Science* **64** 976
[3] Li X J, Geng H B, Lan M J, Yang D Z, He S Y and Liu C M 2010 *Chin. Phys. B* **19** 066103
[4] Li X J, Geng H B, Liu C M, Zhao Z M, Yang D Z and He S Y 2010 *IEEE Transactions on Nuclear Science* **57** 831
[5] Srour J R and Palko J W 2013 *IEEE Transactions on Nuclear Science* **60** 1740
[6] He H, He C H, Zhang J H, Liao W L, Zang H, Li Y H and Liu W B 2020 *Nuclear Engineering and Technology* **52** 1537
[7] Bai Y R, Li Y H, Liu F, Liao W L, He H, Yang W T and He C H 2021 *Acta Phys. Sin.* **70** 172401 (in Chinese)
[8] Messenger S R, Burke E A, Summers G P, Xapsos M A, Walters R J, Jackson E M and Weaver B D 1999 *IEEE Transactions on Nuclear Science* **46** 1595
[9] Dale C, Marshall P, Cummings B, Shamey L and Holland A 1993 *IEEE Transactions on Nuclear Science* **40** 1628
[10] Srour J R, Marshall C J and Marshall P W 2003 *IEEE Transactions on Nuclear Science* **50** 653
[11] Hamedani A, Byggmastar J, Djurabekova F, Alahyarizadeh G, Ghaderi R, Minuchehr A and Nordlund K 2020 *Materials Research Letters* **8** 364
[12] Raine M, Jay A, Richard N, Goiffon V, Girard S, Gaillardin M and Paillet P 2017 *IEEE Transactions on Nuclear Science* **64** 133
[13] Liu Y, Zhu T F, Yao J X and OuYang X P 2019 *Sensors (Basel, Switzerland)* **19** 1767
[14] Shen S S, He C H and Li Y H 2018 *Acta Phys. Sin.* **67** 182401 (in Chinese)
[15] Castellina A and Donato F 2013 *Planets, Stars and Stellar Systems Volume 5: Galactic Structure and Stellar Populations* (Dordrecht: Springer) p. 729
[16] Ziegler J F, Ziegler M D and Biersack J P 2010 *Nuclear Instruments and Methods in Physics Research Section B: Beam Interactions with Materials and Atoms* **268** 1818
[17] Allison J, Amako K, Apostolakis J, *et al.* 2006 *IEEE Transactions on Nuclear Science* **53** 270

[18] Santin G, Ivanchenko V, Evans H, Nieminen P and Daly E 2005 *IEEE Transactions on Nuclear Science* **52** 2294

[19] Ivanchenko V, Apostolakis J, Bagulya A, *et al.* 2011 *Progress in Nuclear Science and Technology* **2** 898

[20] Mendenhall M H and Weller R A 2005 *Nuclear Instruments and Methods in Physics Research Section B: Beam Interactions with Materials and Atoms* **227** 420

[21] Liu H C, Ge W and Wang Y G 2020 *Radiation Effects and Defects in Solids* **176** 441

[22] Cai G B, Yang L and Guo G Q 2017 *Europhys. Lett.* **117** 16001

[23] Krasheninnikov A V, Miyamoto Y and Tománek D 2007 *Phys. Rev. Lett.* **99** 016104

[24] Buchan J T, Robinson M, Christie H J and Roach D L 2015 *J. Appl. Phys.* **117** 245901

[25] Bai X M, Voter A F, Hoagland R G, Nastasi M and Uberuaga B P 2010 *Science* **327** 1631

[26] Whitlow H J and Nakagawa S T 2007 *Nuclear Instruments & Methods in Physics Research* **260** 468